A program to analyse optical coherence tomography images of the ciliary muscle

Deborah S. Laughton[1], Benjamin J. Coldrick[1,2], Amy L. Sheppard[1] & Leon N. Davies[1]

[1] Ophthalmic Research Group, Life & Health Sciences, Aston University, Birmingham, UK

[2] Biomedical Engineering, Life & Health Sciences, Aston University, Birmingham, UK

Corresponding author

Leon N Davies PhD, Ophthalmic Research Group, Life & Health Sciences, Aston University, Birmingham, B4 7ET, UK

Tel: +44(0)121 204 4152

Fax: +44 (0) 121 204 4048

Keywords: Accommodation, AS-OCT, ciliary muscle, presbyopia

Disclosure: The authors report no conflicts of interest and have no proprietary interest in any of the materials mentioned in this article

Acknowledgments: DL is supported by a College of Optometrists Postgraduate Research Scholarship. We would like to acknowledge Ms Naomi Richa Saigal for imaging the rigid gas-permeable lenses.

Abstract

Purpose

To describe and validate bespoke software designed to extract morphometric data from ciliary muscle Visante Anterior Segment Optical Coherence Tomography (AS-OCT) images.

Method

Initially, to ensure the software was capable of appropriately applying tiered refractive index corrections and accurately measuring orthogonal and oblique parameters, 5 sets of custom-made rigid gas-permeable lenses aligned to simulate the sclera and ciliary muscle were imaged by the Visante AS-OCT and were analysed by the software. Human temporal ciliary muscle data from 50 participants extracted via the internal Visante AS-OCT caliper method and the software were compared. The repeatability of the software was also investigated by imaging the temporal ciliary muscle of 10 participants on 2 occasions.

Results

The mean difference between the software and the absolute thickness measurements of the rigid gas-permeable lenses were not statistically significantly different from 0 (t=-1.458, p=0.151). Good correspondence was observed between human ciliary muscle measurements obtained by the software and the internal Visante AS-OCT calipers (maximum thickness t=-0.864, p=0.392, total length t=0.860, p=0.394). The software extracted highly repeatable ciliary muscle measurements (variability $\leq$6% of mean value).

Conclusion

The bespoke software is capable of extracting accurate and repeatable ciliary muscle measurements and is suitable for analysing large data sets.

Introduction

Despite the involvement of the ciliary muscle in accommodation [1-3], presbyopia [4-5], and possibly myopia development [6-9], there is a relative paucity of *in vivo* ciliary muscle research. Indeed, imaging the ciliary muscle *in vivo* represents a significant challenge due to the obscured position of the ciliary muscle behind the highly pigmented iris.

Traditionally, ultrasound biomicroscopy (UBM) has been utilised to acquire *in vivo* images of the ciliary muscle [10-13]. However, sharper image definition obtained with Anterior Segment Optical Coherence Tomography (AS-OCT) permits superior localisation of the scleral spur (a key reference point for ciliary muscle measurements), compared to UBM images [13]. The axial resolution is 8 µm and 25 µm for the Visante AS-OCT (Carl Zeiss Meditec, California, USA) in high resolution corneal mode and the P40 UBM (Paradigm Medical Industries, Utah, USA) at 50 MHz [13], respectively. Additionally, UBM necessitates supine posture, topical anaesthetic, coupling agents and contralateral eye fixation, whereas the Visante AS-OCT permits non-contact ipsilateral imaging of the fixating eye whilst the patient is sitting up-right, which affords enhanced patient comfort and feasibly permits paediatric assessment [2,6]. Therefore more recent research has progressed to use AS-OCT devices rather than UBM to image the ciliary muscle *in vivo* [1-6, 8-9].

Similarly to UBM devices, in-built Visante AS-OCT software allows calipers to be super-imposed onto acquired images to extract measurements. During image analysis, the Visante AS-OCT internal software outlines the boundaries of the ocular media and applies corrective refractive indices (n) to improve measurement accuracy (n=1.000 anterior to the cornea, n=1.338 to the cornea, n=1.343 posterior to the cornea). However, the Visante AS-OCT also fits the same refractive index adjustments to ciliary muscle images, with no option to alter the magnitude of the tiered refractive index corrections. Therefore, previous authors have applied a refractive index of 1.000 to the entire ciliary muscle image [1,4,6]. To provide data more closely associated with physiological *in vivo* ciliary muscle parameters, Sheppard and Davies [1,4] adjusted their ciliary muscle caliper measurements to account for a refractive index of 1.382, which is the best estimate of the refractive index of the ciliary muscle based on *in vitro* bovine muscle tissue studies using confocal microscopy [14] and *in vitro* human ventricular muscle studies using OCT [15]. However, the refractive indices of the overlying sclera, as well as the ciliary muscle itself, need to be compensated for to ensure the magnitude of the measured ciliary muscle parameters are as accurate as possible. Furthermore, the ciliary muscle tissue is not accurately represented by the straight lines of the calipers because the scleral and ciliary muscle tissues are curved, to varying degrees in different patients [16]. Therefore, to improve the accuracy of morphological assessment, data have been exported for analysis with external software [16].

Due to the lack of uniformity of the ciliary muscle outline in Visante AS-OCT images, Kao and colleagues' [16] software required manual localisation of the scleral spur before automated image analysis commenced. Once the sclera and ciliary muscle had been outlined, refractive indices of 1.41 and 1.38 were applied across the y-axis of the scleral and ciliary muscle image sections, respectively. The software produced vertical thickness measures at 1, 2 and 3 mm behind the scleral spur, maximum thickness and measured the cross-sectional area of the anterior ciliary body. However, the edge detection algorithms appeared to incorporate both the ciliary muscle and the pigmented ciliary epithelium, which may overestimate ciliary muscle measurements. Furthermore, measurements of ciliary muscle length were not obtained.

Despite the Visante AS-OCT's use in previous morphometric studies of the ciliary muscle, the instrument remains susceptible to optical and instrument distortions, and has limited inbuilt capabilities to quantify ciliary muscle parameters. Consequently, to overcome the limitations of previously designed software [16] and to address concerns of the subjectivity of identifying the posterior end point of the ciliary muscle [17], bespoke software was developed. The aim of this study was to describe and validate the bespoke software and to compare data extracted by the software and the internal Visante AS-OCT calipers.

Method

The study was approved by the Aston University Research Ethics Committee and was conducted in accordance with the tenets of the Declaration of Helsinki. Informed consent was obtained from all participants after explanation of the nature and possible consequences of the study. One UK registered optometrist (DL) acquired and extracted all the human data.

Ciliary muscle image acquisition

It is likely that the repeatability of nasal ciliary muscle image analysis is superior to temporal ciliary muscle image analysis because the scleral spur is more easily discernible nasally [18], therefore only temporal ciliary muscle images were analysed in the present study.

Each participant wore an eye patch over their left eye throughout data collection. Participants were asked to place their chin and forehead against the Visante AS-OCT supports and fixate straight-ahead at the centre of the internal star target. The chin rest was adjusted to align the participant's right eye to allow visualisation of the anterior crystalline lens surface, which was guided by the real-time Visante AS-OCT video stream of the external eye. High resolution corneal mode was selected (scanning an area of 10 mm in width and 3 mm in depth) and participants were aligned to ensure the vertical white fixation line was visible through the centre of the image, which indicated the measurement beam was coincident with the optical axis of the eye [19].

In order to image the full length of the ciliary muscle using the Visante AS-OCT, patients must avert their gaze to a point external to the central viewing window because the iris blocks visualisation of the ciliary muscle in primary gaze. Fig. 1 illustrates the bespoke Badal lens system with a moveable Maltese cross target, attached to the forehead rest of the Visante AS-OCT to provide a steady peripheral fixation target and to correct for ametropia. The minimum level of horizontal eye movement required to ensure the peripheral target is unobstructed by the instrument casing is 40^{o} from the internal Visante AS-OCT star target. Fixating externally causes the Visante AS-OCT beam to be directed through the sclera, rather than the cornea, reducing optical distortion due to the flatter scleral plane. Since all participants were aligned to the optical axis of the Visante AS-OCT in primary position, only minor vertical alignment adjustments were required once the participant adducted their right eye to view the centre of the external Maltese cross. Horizontal alignment was determined by the real-time Visante AS-OCT video stream of the OCT image, which was adjusted to ensure simultaneous visualisation of the scleral spur and ciliary muscle posterior visible limit, as depicted in Fig. 2.

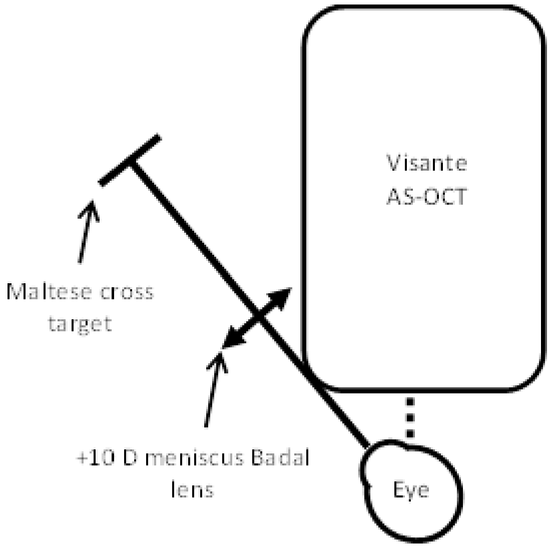

Fig. 1. Schematic diagram of the Visante AS-OCT with bespoke Badal lens system attachment. The dashed line represents the path of the OCT beam through the sclera. The Maltese cross target is positioned 10 cm from the Badal lens in order to stimulate 0.00 D of accommodation in an emmetropic patient.

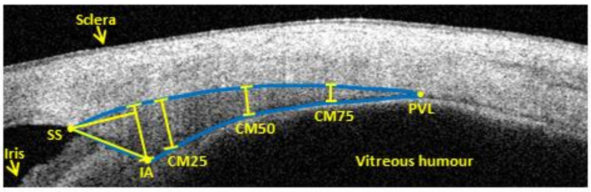

Fig. 2. Visante AS-OCT image of a human ciliary muscle section. The ciliary muscle is outlined in blue with superimposed yellow caliper measurements. PVL = posterior visible limit; SS = scleral spur; IA = inner apex; CM25, CM50, CM75 = thickness at 25%, 50% and 75% of curved total length (SS to PVL); maximum thickness = perpendicular distance from IA to sclera; anterior length = perpendicular distance from line of maximum thickness to SS. The pigmented epithelium is visible underneath the inner apex and the inferior ciliary muscle border.

Once accurately aligned, the Maltese cross target was moved to provide a 0.00 D accommodative stimulus for each participant. Participants were asked to focus on the centre of the Maltese cross target and keep it as clear as possible throughout data collection, whilst also keeping their head and eyes as still as possible. Three consecutive images of the right eye temporal ciliary muscle were acquired and saved.

Software design

The preparation of ciliary muscle images for analysis was similar to the process used by Kao *et al*. [16]; all images acquired in high resolution corneal mode were exported in raw DICOM (Digital Imaging and Communications in Medicine) form (n=1.00) and were imported to Matlab R2012b (The MathWorks Inc., Massachusetts, USA) and subsequently resized to 512 x 1280 pixels, matching the correct aspect ratio. The images were not cropped or reduced in size for processing.

Due to the difficulties in localising the outline of the ciliary muscle, the bespoke software required multiple landmarks to be manually selected before extracting data. Initially, the scleral spur and a point beyond the posterior visible limit were selected manually (highlighted by yellow dots in Fig. 3A). The software then calculates the distance between these two markers and superimposes a vertical line midway, prompting the user to pick the points where the scleral/ciliary muscle and ciliary muscle/pigmented ciliary epithelium boundaries bisect the line. These initial steps identify the area of interest to the software, which then superimposes a block of 10 vertical lines spaced at 1 pixel intervals every 0.5 mm between the scleral spur and posterior point chosen. The change in pixel intensity along each line is determined. To define the ciliary muscle border, a 2nd order Fourier series is fitted to the intensity profile and differentiated. The location of the largest peak formed in the differentiated intensity profile corresponds to the point where the line bisects the ciliary muscle boundary (the crossing point). This process is repeated for the top and bottom of each line separately in order to determine crossing points of both the superior and inferior ciliary muscle boundaries on the OCT image. A 2nd order polynomial curve is fitted to the crossing points of each boundary.

The ciliary muscle/pigmented ciliary epithelium border is not as easily discriminated as the scleral/ciliary muscle border, therefore the software provides an option to manually pick three points along the boundary to improve the fit of the curve, if the automated fit is not satisfactory (Fig. 3B). Due to relatively poor image clarity around the inner apex of the ciliary muscle, the inner apex must also be selected manually. Once the fit of the curves to the ciliary muscle borders has been finalised, the OCT image is converted to a binary image in order for internal MatLab edge detection algorithms to identify the air/scleral boundary and fit a 2nd order polynomial curve to it. During software development and testing, it was determined that 2nd order curves accurately and satisfactorily fitted the contour of the ciliary muscle and sclera in all patients tested.

Subsequently, the software applies a tiered refractive index correction to the scleral and ciliary muscle tissue (1.41 and 1.38, respectively), as shown in Fig. 3C by the higher yellow and green curves. The posterior visible limit of the ciliary muscle is identified as the point where the curves fitted to the ciliary muscle borders reach minimum separation posteriorly. The software exports the Straight-line TL (straight-line distance between the scleral spur and posterior visible limit), Curved TL (ciliary muscle total length measured along the scleral/ciliary muscle boundary), Max T (maximum thickness; see Fig. 2), Ant L (anterior length measured perpendicularly from the line of maximum thickness to the scleral spur), SS-IA (distance between scleral spur to the inner apex), CM2 (thickness measured 2 mm from the scleral spur along the scleral curve), CM25 (thickness measured at 25% of the total curved length of the ciliary muscle), CM50 (thickness measured at 50% of the total curved length of the ciliary muscle) and CM75 (thickness measured at 75% of the total curved length of the ciliary muscle), directly to an Excel spreadsheet, allowing the examiner to be masked to the results.

Due to the uncertainties of measuring thickness at fixed distances from the scleral spur, which is likely to represent a different anatomical area of the ciliary muscle between subjects, CM1 (thickness measured 1 mm behind the scleral spur along the scleral curve) and CM3 (thickness measured 3 mm behind the scleral spur along the scleral curve) were not quantified. However, CM2 was included due to the hypothesis this area may act as a fulcrum point during accommodation, where the net change in thickness is negligible [2].

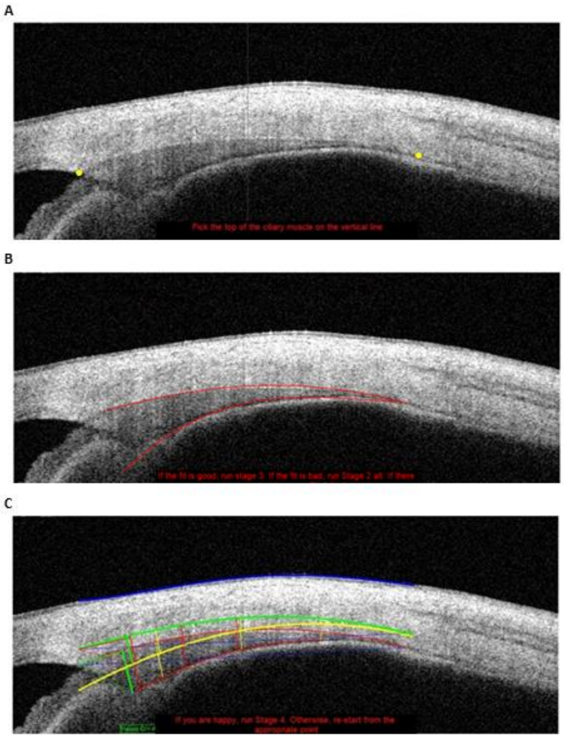

Fig 3. A) Screenshot from the software after the scleral spur and a point beyond the posterior visible limit (yellow dots) have been clicked on. The user is required to select where the top and bottom ciliary muscle boundaries are bisected by the superimposed vertical line. B) The software outlines the boundaries of the ciliary muscle and gives the option to manually redefine the lower curve. C) After manually selecting the inner apex the software extracts the ciliary muscle data, correcting for the refractive indices of the sclera and ciliary muscle (higher yellow and green curves) and transfers the data to an Excel document.

Software analysis of artificial ciliary muscle sections

To ensure the software was capable of appropriately applying refractive index corrections and accurately measuring orthogonal and oblique parameters, a series of custom-made rigid gas-permeable lenses (No. 7 Contact Lens Laboratory Ltd, Hastings, UK) of known dimensions were imaged by the Visante AS-OCT. One silicon-acrylate lens (n= 1.48) simulated the sclera (L_1 in Fig. 4) and 5 fluoro-polymer lenses (n=1.44) of varying thickness (0.3, 0.45, 0.6, 0.75, 0.9 mm) each simulated the ciliary muscle (L_2 in Fig. 4). Each of the ciliary muscle lenses were of constant thickness. The total diameter of the sclera lens was 10 mm and each ciliary muscle lens was 6 mm. The radius of curvature of the lenses was 12 mm. A ciliary muscle lens and the sclera lens were positioned together, as shown in Fig. 4, for image acquisition. For each of the 5 ciliary muscle and sclera lens combinations, 10 OCT images were acquired and exported as raw data.

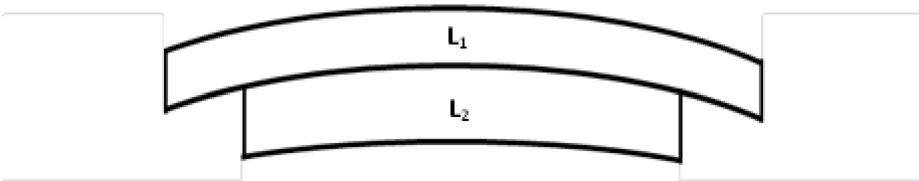

Fig. 4. Schematic diagram of two rigid gas-permeable lenses designed to simulate the sclera (L_1) and the ciliary muscle (L_2).

For this exercise only, the ciliary muscle software was adapted to allow 3 points across each of the lens boundaries to be manually selected for subsequent automated polynomial curve (order 2) fitting. The software determines the length of the ciliary muscle lens as the straight-line distance between the first and third points plotted across the scleral/ciliary muscle boundary, therefore the edges of the lens were manually selected. The thicknesses of the ciliary muscle lenses were measured at 25 (CM25), 50 (CM50) and 75% (CM75) across the lens diameter. Each thickness measurement was measured perpendicular to the scleral/ciliary muscle boundary curve. The refractive indices of the scleral and ciliary muscle lenses (1.48 and 1.44, respectively) were inputted to allow the program to compensate the measurements. All measurements were exported directly to an Excel spreadsheet, masking the examiner to the results during data extraction. The diameter and thickness measurements of the ciliary muscle lenses were also measured 10 times by Vernier calipers and compared to the results produced by the software.

The bias of the measurements was calculated from the mean difference between the two techniques. A paired t-test was used to determine whether the bias was significantly different from

0. The spread over which 95% of the data lie (limits of agreement, LoA) was calculated and the agreement of the software and Vernier calipers was analysed using a Bland-Altman plot [20].

Software and Visante AS-OCT caliper agreement

Human ciliary muscle parameters acquired by the software were compared to those acquired via the traditional method of ciliary muscle Visante AS-OCT image analysis: internal Visante AS-OCT calipers. Disaccommodated temporal ciliary muscle images of 50 patients (mean age 39.11 ± 3.18 years; mean spherical equivalent -1.17 ± 2.09 D, range -7.07 to +0.49 D; mean astigmatism -0.59 ± 0.57 D) were acquired and data were subsequently extracted by the software and the Visante AS-OCT calipers on separate occasions.

The software was designed to measure the ciliary muscle thickness with reference to the curved ciliary muscle length (following the contour of the scleral/ciliary muscle border), whereas the Visante AS-OCT calipers cut across the ciliary muscle to measure its thickness at horizontal distances from the scleral spur. Therefore, the calipers are likely to underestimate the thickness measurements in a more curved ciliary muscle [6,16]. Due to the aforementioned differences in the origin of thickness measurements from the scleral spur, only the Straight-line TL and Max T measurements were compared between the two methods. The software Straight-line TL and the software Curved TL values were also compared.

Internal Visante AS-OCT caliper measurements were acquired by applying a refractive index of 1.00 to the entire image and superimposing calipers on to the ciliary muscle image to extract Straight-line TL and Max T measurements. For comparison with the internal Visante AS-OCT caliper measurements, the software was adapted to export the raw ciliary muscle measurements with a refractive index of 1.00 applied to the entire image.

The bias was calculated from the mean difference between the techniques and a paired t-test was used to determine whether the bias was significantly different from 0. The agreement of the techniques was also analysed using Bland-Altman plots. The difference between the software Straight-line TL and the software Curved TL values was analysed using a paired t-test.

Repeatability of software analysis of human ciliary muscle

Additionally, the repeatability of human ciliary muscle OCT imaging and software interpretation was determined by inviting 10 participants to return for ciliary muscle imaging on a separate occasion, less than 1 week after their first appointment. A further three ciliary muscle images were acquired and analysed.

In order to determine the errors arising from patient alignment and software interpretation, the ciliary muscle of a single patient's right eye was imaged 10 times at 0.00 D accommodative stimulus during one appointment. The patient was asked to remove and reposition their chin and forehead between the acquisition of each image. In order to isolate the repeatability of the software interpretation and analysis of a ciliary muscle image, 1 image was analysed 10 times.

The bias of each parameter was calculated from the mean difference between visits. A paired t-test was used to determine whether the bias was significantly different from 0.

Results

Artificial ciliary muscle sections

The mean difference between the software and the Vernier caliper measurements are displayed in Table 1. The bias of CM25, CM50 and CM75 were not significantly different from 0. The bias was not correlated with the magnitude of the measurement. However the total diameter was significantly underestimated by the software (p=0.001).

Software and caliper agreement

The mean difference between the software and the Visante AS-OCT internal caliper total Straight-line TL and Max T measurements are displayed in Table 2. The bias of each parameter was not significantly different from 0. The data are displayed graphically with Bland-Altman plots in Figs 5 and 6, which show the bias was not correlated to the magnitude of the measurement. The mean software Curved TL measurements (5.391 ± 0.571 mm) were significantly longer than the mean software Straight-line TL measurements (5.301 ± 0.560 mm; t=-23.356, p<0.001).

A

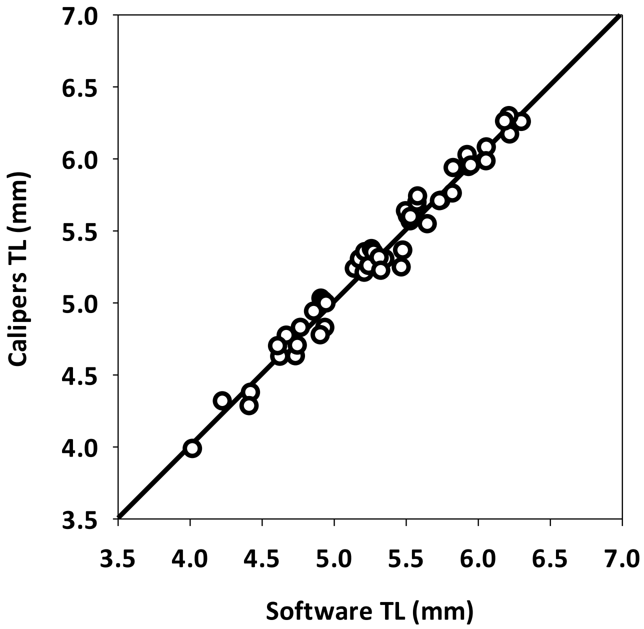

B

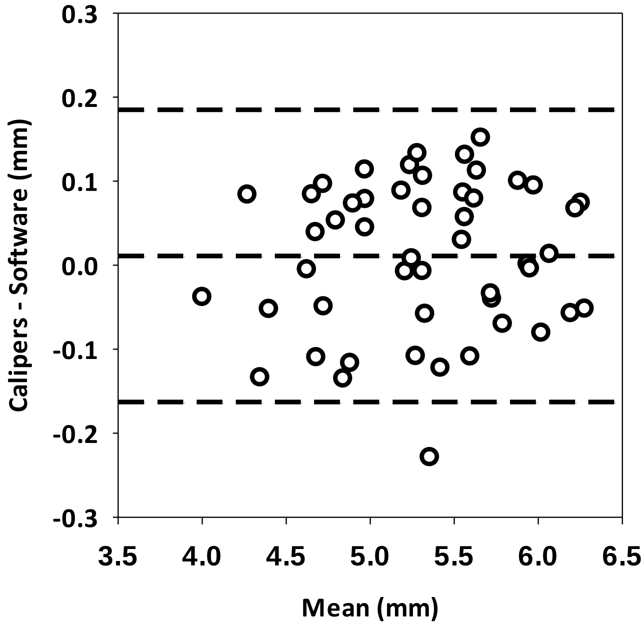

Fig. 5. A. Total straight-line length measured by the software and the internal Visante AS-OCT calipers. Regression line y=0.132+0.973x, R^2=0.876, p<0.001. **B.** Bland-Altman plot of the agreement between total straight-line length measured by the software and the internal Visante AS-OCT

calipers. Regression line y=-0.068+0.015x, R^2=0.009, *p*=0.514. The dashed lines represent the limits of agreement.

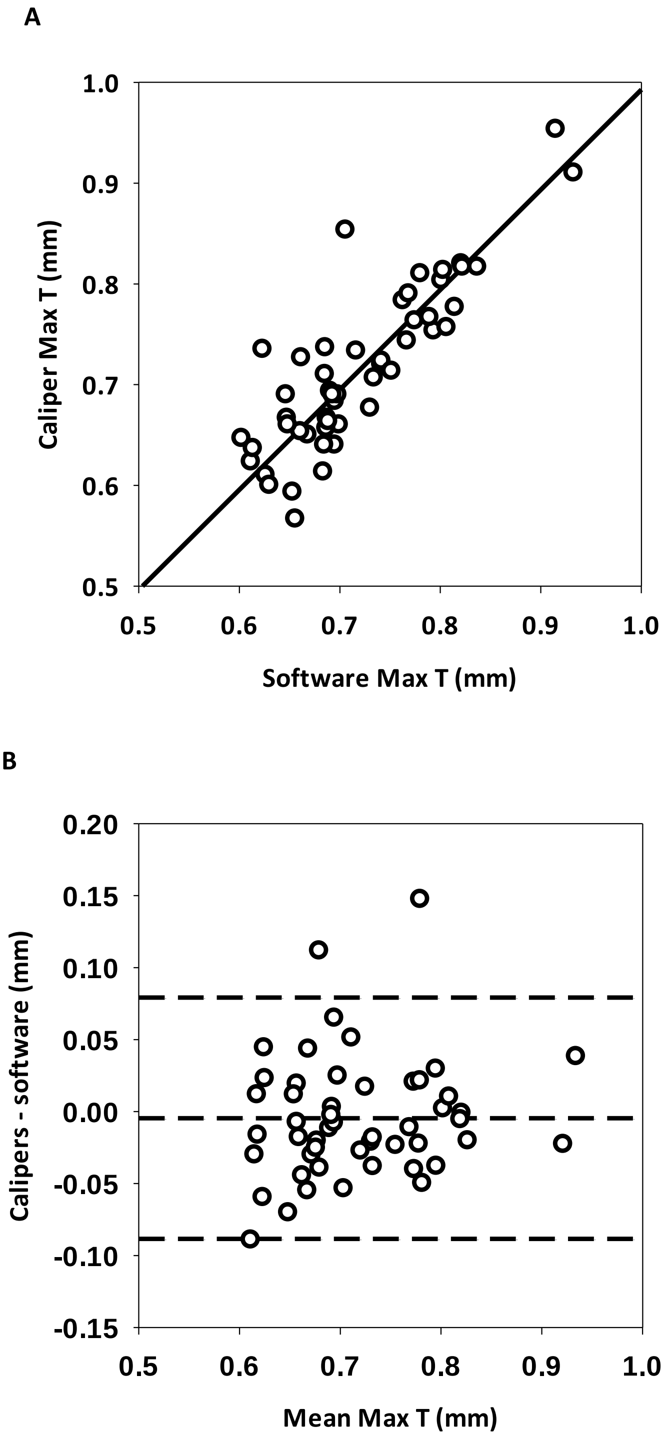

Fig. 6. A Maximum thickness measured by the software and the internal Visante AS-OCT calipers. Regression line y=0.152+0.794x, R^2=0.732, *p*<0.001. **B.** Bland-Altman difference versus mean plot of the agreement between maximum thickness measured by the software and the internal Visante AS-

OCT calipers. Regression line y=-0.063+0.081x, R^2=0.021, p=0.317. The dashed lines represent the limits of agreement.

Repeatability

The bias of ciliary muscle parameters measured in 10 patients across 2 visits is displayed in Table 3. The bias represented $\leq$6% of the mean value of each parameter and was not significantly different from 0. Tables 4 and 5 obtained from 1 patient realigned 10 times and 1 image analysed 10 times, respectively, suggest approximately 60% of the difference encountered between visits is likely to be due to the inherent variability associated with manually selecting points for analysis with the bespoke software.

Discussion

The software described here is capable of accurately outlining the ciliary muscle, applying appropriate refractive index corrections and extracting a variety of repeatable orthogonal and oblique ciliary muscle parameters, thus verifying its suitability for *in vivo* ciliary muscle analysis. Compared to the Visante AS-OCT calipers, the software enables more accurate measurements of the curved ciliary muscle tissue to be acquired by following the scleral/ciliary muscle contour, rather than cutting horizontally across the ciliary muscle to measure thicknesses with respect to the distance from scleral spur. Image analysis can also be performed remotely to the Visante AS-OCT device on an external computer. As with the Visante AS-OCT's calipers, the bespoke software is not fully automated and requires user input at various stages of the analysis.

The software raw parameters (n=1.00) compared favourably to internal Visante AS-OCT caliper Straight-line TL and Max T measurements, suggesting the location of the posterior visible limit, utilised in the total length measurement, is not only evident across a large sample of patients, but can also be consistently identified subjectively and objectively. Nevertheless, the concerns of previous authors over the visibility of the posterior end point of the ciliary muscle are not entirely unfounded [17]; extensive analysis of ciliary muscle images during software development has shown there is large intersubject variability in the visibility of the posterior limit of the ciliary muscle. In order to simplify localisation for the software, the posterior visible limit was defined as the point where the scleral/ ciliary muscle and ciliary muscle/ pigmented ciliary epithelium contours reached minimum separation posteriorly, which produced highly repeatable results.

Orthogonal and oblique thickness measurement accuracy was evidenced by computation of the distance between 2 polynomial curves (order 2) fitted to OCT images of 2 superimposed rigid gas-permeable lenses. As expected, the total diameter measurements were significantly underestimated by the software (p=0.001) due to difficulties ensuring the scleral and ciliary muscle lenses were perfectly centred, and that the measurement beam scanned across the centre of both lenses. Nonetheless, the validity of horizontal measurements has been confirmed by the good correspondence between the internal Visante AS-OCT caliper and the software Straight-line TL measurements. The thickness measurements obtained are unaffected by the aforementioned alignment issues because all the ciliary muscle lenses were of constant thickness.

The agreement between the ciliary muscle lens thickness values measured by the software and Vernier calipers demonstrates the software can appropriately compensate for tiered refractive index levels and the geometric distortion of the exported image in raw DICOM form is negligible. These findings also support the conclusions of Kao *et al.* [16], who reported images exported from the Visante AS-OCT images are free from geometric distortions and only need to be adjusted for the refractive index of the tissue(s) to be suitable for accurate morphological assessment.

The bias and variance of the difference in ciliary muscle parameters extracted from 10 patients on 2 separate visits was similar to internal Visante AS-OCT caliper measurement values reported previously [1]. Furthermore, the limits of agreement reported by the software (-0.166 to 0.135 mm) were narrower than for the calipers (-0.228 to 0.193 mm) for the measurement of total straight-line length, suggesting superior repeatability of the localisation of the posterior visible limit by the software. The intersession repeatability of the software developed by Kao and colleagues [16] was not reported.

It is unlikely fully-automated software could be developed to analyse the current ciliary muscle images produced by the Visante AS-OCT due to the non-uniformity of the acquired image. A custom-made OCT instrument has been able to obtain sharper definition around the inner apex of the ciliary muscle, however manual selection of key landmarks is still required to initiate image analysis [21].

The newly developed software described by the current study extracts valid and repeatable ciliary muscle parameters and serves to reduce the subjectivity of ciliary muscle analysis. The image examiner must be highly trained to extract repeatable results due to the ambiguity of ciliary muscle landmarks in some patients. The software described here also has the capacity to extract a variety of additional measurements to previous software [16], including ciliary muscle length, which is a vital measurement for presbyopia research [16].

References

[1] Sheppard AL, Davies LN. In vivo analysis of ciliary muscle morphologic changes with accommodation and axial ametropia. Invest Ophthalmol Vis Sci. 2010; 51: 6882-9

[2] Lewis HA, Kai C, Sinnott LT, Bailey MD. Changes in ciliary muscle thickness during accommodation in children. Optom Vis Sci. 2012; 89(5): 727-37

[3] Lossing LA, Sinnott LT, Kai C, Richdale K, Bailey MD. Measuring changes in ciliary muscle thickness with accommodation in young adults. Optom Vis Sci. 2012; 89(5): 719-26

[4] Sheppard AL, Davies LN. The effect of ageing on in vivo human ciliary muscle morphology and contractility. Invest Ophthalmol Vis Sci. 2011; 52: 1809-16

[5] Richdale K, Sinnott LT, Bullimore MA, Wassenaar PA, Schmalbrock P, Kao CY *et al.* Quantification of age-related and per diopter accommodative changes of the lens and ciliary muscle in the emmetropic human eye. Invest Ophthalmol Vis Sci. 2013; 54(2): 1095-105

[6] Bailey MD, Sinnott LT, Mutti DO. Ciliary Body Thickness and Refractive Error in Children. Invest Ophthalmol Vis Sci. 2008; 49: 4352-60

[7] Jeon S, Lee WK, Lee K, Moon NJ. Diminished ciliary muscle movement on accommodation in myopia. Exp Eye Res. 2012; 105: 9-14

[8] Buckhurst H, Gilmartin B, Cubbidge RP, Nagra M, Logan NS. Ocular biometric correlates of ciliary muscle thickness is human myopia. Ophthal Physiol Opt. 2013;33(3):294-304

[9] Pucker AD, Sinnott LT, Kao C, Bailey MD. Region specific relationships between refractive error and ciliary muscle thickness in children. Invest Ophthalmol Vis Sci. 2013; 54: 4710-6

[10] Oliveira C, Tello C, Liebmann JM, Ritch R. Ciliary body thickness increases with increasing axial myopia. Am J Ophthalmol. 2005; 140(2): 324-5

[11] Muftuoglu O, Hosal BM, Zilelioglu G. Ciliary body thickness in unilateral high axial myopia. Eye. 2009; 23(5): 1176-81

[12] Jeon S, Lee WK, Lee K, Moon NJ. Diminished ciliary muscle movement on accommodation in myopia. Exp Eye Res. 2012; 105: 9-14

[13] Dada T, Sihota R, Gadia R, Aggarwal A, Mandal S, Gupta V. Comparison of anterior segment optical coherence tomography and ultrasound biomicroscopy for assessment of the anterior segment. J Cataract Refract Surg. 2007; 33: 837-40

[14] Dirckx JJ, Kuypers LC, Decraemer WF. Refractive index of tissue measured with confocal microscopy. J Biomed Opt. 2005; 10(4): 0440141-0440148

[15] Tearney GJ, Brezinski ME, Southern JF, Bouma BE, Hee MR, Fujimoto JG. Determination of the refractive index of highly scattering human tissue by optical coherence tomography. Opt Lett. 1995; 20: 2258-61

[16] Kao CY, Richdale K, Sinnott LT, Grillott LE, Bailey MD. Semiautomatic extraction algorithm for images of the ciliary muscle. Optom Vis Sci. 2011; 88: 275-89

[17] Bailey MD. Letter: How should we measure the ciliary muscle? Invest Ophthalmol Vis Sci. 2011; 52: 1817–8

[18] Sakata LM, Lavanya R, Friedman DS, Aung HT, Seah SK, Foster PH et al. Assessment of the scleral spur in anterior segment optical coherence tomography images. Arch Ophthalmol. 2008; 126(2): 181-5

[19] Richdale K, Bullimore MA, Zadnik K. Lens thickness with age and accommodation by optical coherence tomography. Ophthal Physiol Opt. 2008; 28: 441-7

[20] Bland JM, Altman DG. Statistical methods for assessing the agreement between two methods of clinical measurement. Lancet. 1986; 327(8476): 307-10

[21] Ruggeri M, Hernandez V, Freitas C, Manns F, Parel JM. Biometry of the ciliary muscle during dynamic accommodation assessed with OCT. Proc SPIE 8930, Ophthalmic Technologies XXIV, 89300W. 2014; doi: 10.1117/12.2044309

Table 1. Comparison of parameters obtained from 5 artificial ciliary muscle sections by the software and Vernier calipers. A negative mean difference indicates the software values are larger than the Vernier caliper measurements.

Parameter	Mean difference (mm)	Standard deviation (mm)	Limits of agreement		t	*p*
			Lower (mm)	Upper (mm)		
Total diameter	0.046	0.092	-0.135	0.226	3.507	0.001
CM25	-0.001	0.017	-0.034	0.032	-0.427	0.671
CM50	-0.003	0.016	-0.034	0.028	-1.458	0.151
CM75	0.000	0.016	-0.031	0.031	-1.810	0.857

Table 2. Comparison of ciliary muscle parameters obtained from 50 patients by the software and the internal Visante AS-OCT calipers. A negative mean difference indicates the software values are larger than the caliper measurements.

Parameter	Mean difference (mm)	Standard deviation (mm)	Limits of agreement		*t*	*p*
			Lower (mm)	Upper (mm)		
Straight-line TL	0.011	0.089	-0.163	0.185	0.860	0.394
Max T	-0.005	0.043	-0.089	0.079	-0.864	0.392

Table 3. Intersession repeatability data of ciliary muscle parameters extracted by the software from 2 visits of 10 patients. A negative mean difference indicates the measurement was larger at visit 1.

Parameter	Mean difference (mm)	Standard deviation (mm)	Limits of agreement		t	*p*
			Lower (mm)	Upper (mm)		
Straight-line TL	-0.016	0.077	-0.166	0.135	-0.569	0.583
Curved TL	-0.017	0.072	-0.157	0.124	-0.736	0.480
Max T	-0.003	0.022	-0.047	0.040	-0.281	0.785
Ant L	0.011	0.059	-0.104	0.126	0.577	0.578
SS-IA	0.007	0.054	-0.099	0.112	0.354	0.731
CM2	-0.007	0.030	-0.066	0.051	-0.761	0.466
CM25	-0.003	0.018	-0.038	0.033	-0.832	0.427
CM50	0.004	0.023	-0.041	0.050	0.535	0.606
CM75	0.009	0.020	-0.030	0.048	1.335	0.215

Table 4. Ciliary muscle parameters extracted by the software from 10 images acquired from one patient who removed and repositioned their head between acquisitions.

Parameter	Mean (mm)	Standard deviation (mm)
Straight-line TL	5.164	0.068
Curved TL	5.228	0.075
Max T	0.482	0.014
Ant L	1.182	0.043
SS-IA	1.254	0.052
CM2	0.345	0.025
CM25	0.475	0.016
CM50	0.261	0.015
CM75	0.114	0.015

Table 5. Ciliary muscle parameters extracted by the software from one image analysed 10 times.

Parameter	Mean (mm)	Standard deviation (mm)
Straight-line TL	5.153	0.043
Curved TL	5.218	0.038
Max T	0.454	0.011
Ant L	1.237	0.021
SS-IA	1.276	0.040
CM2	0.334	0.016
CM25	0.456	0.008
CM50	0.259	0.006
CM75	0.121	0.011